Eur. Phys. J. Appl. Phys. **51**, 33212 (2010)
DOI: 10.1051/epjap/2010112

THE EUROPEAN PHYSICAL JOURNAL APPLIED PHYSICS

Regular Article

On physical properties of undoped and Al and In doped zinc oxide films deposited on PET substrates by reactive pulsed laser deposition

M. Girtan[1], M. Kompitsas[2,a], R. Mallet[3], and I. Fasaki[2]

[1] Université d'Angers, Laboratoire POMA, CNRS FRE 2988, 2 boulevard Lavoisier, 49045 Angers, France
[2] National Hellenic Research Foundation, LATA Laboratory, Athens, Greece
[3] SCIAM, Université d'Angers, France

Received: 12 October 2009 / Accepted: 14 June 2010
Published online: 2 September 2010 –

Abstract. Undoped and Al and In doped ZnO films were deposited on flexible PET substrates by Reactive Pulsed Laser Deposition (R-PLD). The morphological and structural characteristics of the obtained structures were investigated by AFM, SEM and XRD respectively. The transmittance spectra were recorded in the 300–1200 nm wavelength range and the electrical conductivity was measured. The samples appeared as granular and polycrystalline with high transparency and had a good electrical conductivity. The crystallinity of the undoped ZnO films improved with increasing pressure of the reactive oxygen gas. Doping of ZnO with Al or In modified the energy band gap and the resistivity of the material. The possibility for the application of such structures for the development of hybrid photovoltaic cells on flexible substrates will be demonstrated.

1 Introduction

For the development of organic and flexible electronics, optically transparent plastics with high glass transition temperatures are desired for many optoelectronic devices such as: organic solar cells (OSC), organic light emitting diodes (OLED) or organic field effect transistors (OFET). Polyethylene terephthalate (PET) has been widely used as a substrate material for the growth of transparent conducting oxide thin films as electrodes [1–4]. At present, ITO (tin-doped indium oxide) is mostly used as the transparent electrode for such applications. Due to the high cost of Indium and its reduced abundance, recent research has focused on zinc oxide (ZnO) as a possible replacement of ITO.

Various deposition methods of zinc oxide films on glass substrates were used [5–9], such as thermal oxidation, spray pyrolysis, sputtering, etc. Pulsed laser deposition (PLD) is considered as an efficient method for depositing doped ZnO films with controlled stoichiometry [10]. In particular, there is a strong correlation between the energetic plasma created by the pulsed laser and the oxygen pressure [11], but the main advantage is the deposition of a variety of doped films at low temperatures.

In this paper, we report on the surface morphology and the optical, structural and electrical properties of undoped and Al:ZnO (AZO) and In:ZnO (IZO) doped thin films, deposited by reactive pulsed laser deposition (R-PLD).

[a] e-mail: michael.kompitsas@gmail.com

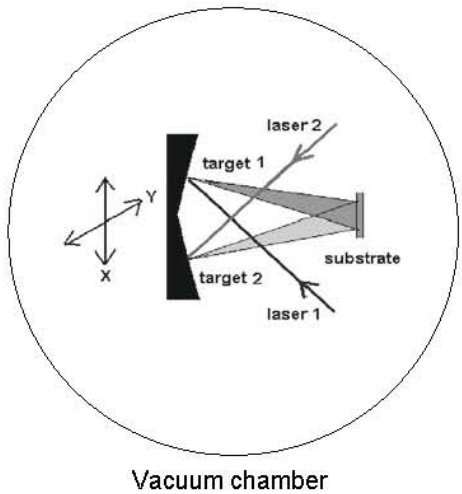

Fig. 1. Pulsed laser deposition setup.

2 Experimental

The experimental setup is schematically shown in Figure 1. All ZnO thin films were deposited on PET substrates (heated at 120 °C) at 10, 20, and 30 Pa oxygen pressures for 1.5 h. For the undoped ZnO films, only the 248 nm excimer laser was employed for the ablation of the ceramic ZnO target. For the Al- and In-doped samples, a second, synchronized 355 nm Nd:YAG laser was used for the ablation of the metallic Al and In targets. The fluence

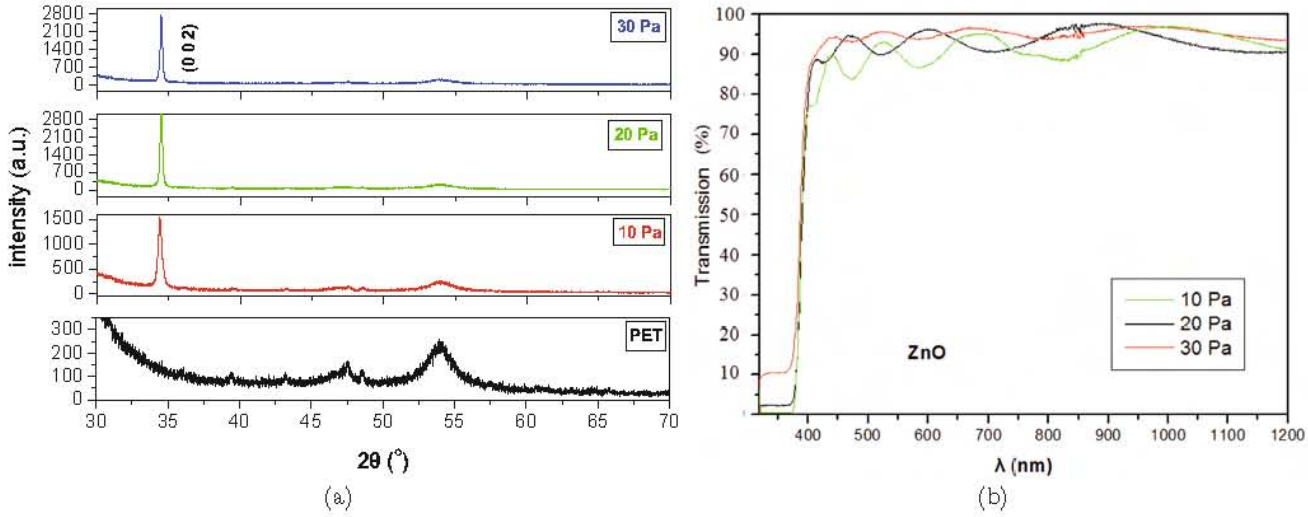

Fig. 2. (Color online) (a) XRD patterns of undoped ZnO films deposited at different oxygen pressures, (b) transmission for undoped ZnO films deposited at different oxygen pressures.

of the second "dopant" laser was varied between 0.7 and 3.4 J/cm^2 and thus the concentration of the dopants in the ZnO film matrix could be controlled. The repetition rate of both lasers was 10 Hz.

The structural characteristics were studied by Cu-K_α (λ = 1.5406 Å) X-ray diffractometry (XRD). The films surface morphology was determined by scanning electron microscopy (SEM) and by atomic force microscopy (AFM). The transmittance spectra were recorded in the wavelength range 300–1200 nm at room temperature, using a Lambda 19 UV-Vis spectrophotometer.

3 Results and discussions

3.1 Undoped ZnO films

The characteristics of the undoped ZnO films at 2.4 J/cm^2 excimer laser fluence have been investigated as a function of the reactive oxygen gas pressure. From the XRD patterns (Fig. 2a) it resulted that the film crystallinity improved for 30 Pa oxygen pressure. From the normalized transmission spectra (Fig. 2b) it followed that the transmission also improved with oxygen pressure, with the 30 Pa sample having an average value close to 90%. The films thickness is given in Table 1. These values followed from the transmission spectra by using the formula of Manifacier et al. [12]:

$$t = \frac{M\lambda_1\lambda_2}{2(n(\lambda_1)\lambda_2 - n(\lambda_2)\lambda_1)}$$

where λ_1 and λ_2 are the wavelength values corresponding to two extrema (minima or maxima) of the transmission curve, $n(\lambda_1)$ and $n(\lambda_2)$ the indices of refraction respectively. The n values have been calculated by using the Sellmeier equation with parameters from [13] and M is 1 for two subsequent 1 extrema. The values given in Table 1 are the average values from various combinations of extrema pairs. We notice that the film at 30 Pa shows a slightly higher average transmission. Together with the XRD results it follows that this sample shows both a better crystallinity and stoichiometry.

Table 1. Undoped ZnO (for 2.4 J/cm^2 of the 248 nm laser).

Oxygen pressure (Pa)	Thickness (nm)
10	547 +/− 10
20	480
30	540

Low resolution SEM images (not presented here) have shown droplets and particulates with irregular shapes on the film surface with sizes of some micrometers. Such μm-sized particles were strongly reduced with the increase of the oxygen pressure. On the other side, the ZnO crystallites were of the order of 100 nm (Fig. 3a), presenting a very regular granular and smooth (RMS = 7 nm) film surface. For comparison, a 3D image of the PET substrate (RMS 8.7 nm) is also presented in Figure 3d. Consequently, we used 30 Pa oxygen pressure for the deposition of the subsequent doped samples.

3.2 Doped ZnO films

To further decrease the number of the μm-sized particles on the doped samples, we reduced the fluence of the 248 nm laser to ca. 2 J/cm^2. This was achieved by placing the focusing lens ca. 10 mm closed to the target: thus, the ablated target area increased while the pulse energy remained the maximum one available.

The XRD patterns are presented in Figure 4a. In the spectrum of the undoped ZnO sample (reference sample for 2 J/cm^2 of the 248 nm laser), we observed the substrate (PET) as well as the well-known (002) plane of ZnO.

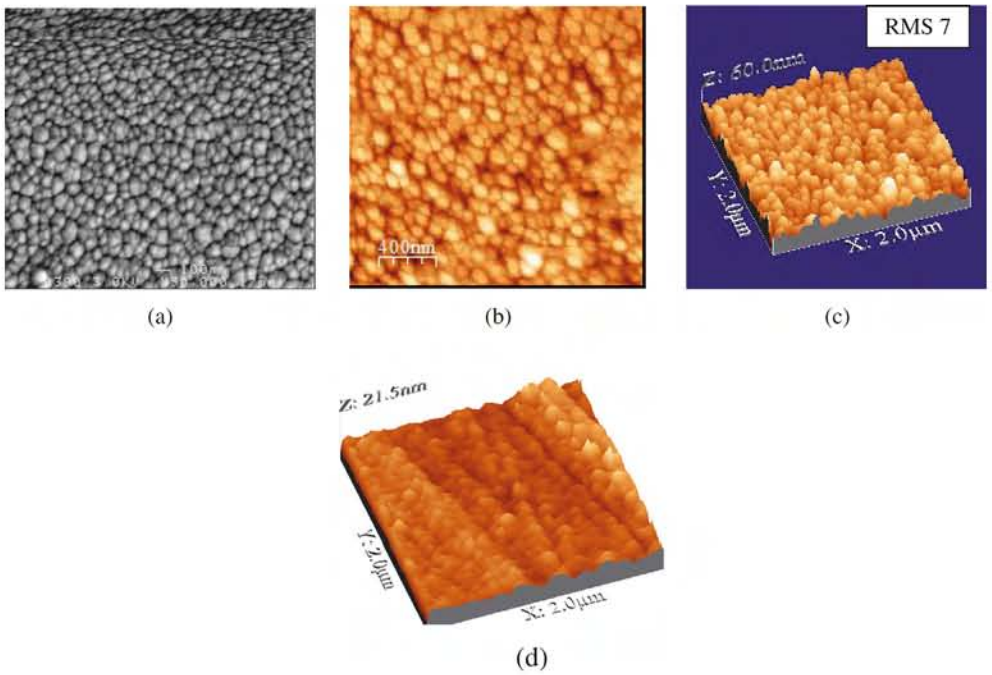

Fig. 3. (Color online) Undoped ZnO sample at 30 Pa: (a) SEM and (b) 2D and (c) 3D AFM micrographs. (d) The 3D AFM image of the PET substrate is shown for comparison.

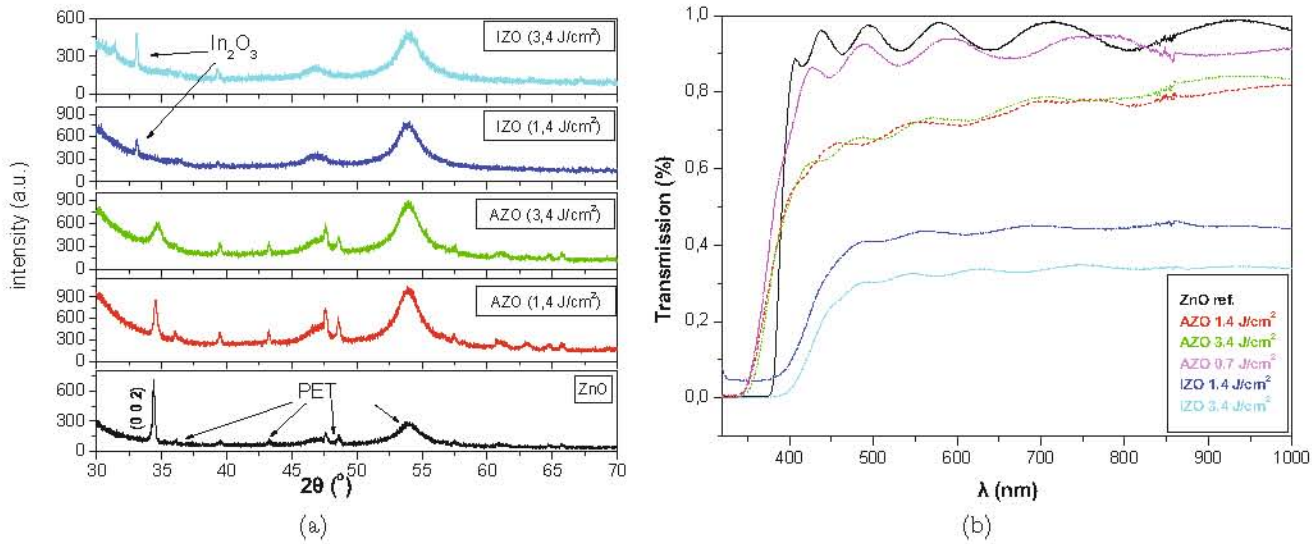

Fig. 4. (Color online) (a) XRD patterns of undoped and Al and In doped zinc oxide films deposited for two fluences of doping laser 1.4 J/cm^{2}and 3.4 J/cm^2, (b) transmission for undoped and Al and In doped ZnO films deposited using different fluences of dopant laser.

The employment of the second "dopant" laser resulted to very different observations for the two dopants. For the Al-doped ZnO (AZO), the crystallinity degrades with the increase of the second laser fluence, as can be seen from the broadening, shifting and decreasing of the (002) ZnO peak. No Al_2O_3 have been observed either. This means that Al is incorporated into the ZnO lattice, replacing Zn sites. We made a similar observation in the past [14]. On the contrary, for the In-doped ZnO (IZO) films, the presence only of the In_2O_3 peaks indicated that the film crystallized rather well as a In_2O_3 matrix that is doped by Zn. This may be the result of the reduced 248 nm laser fluence for the Zn target and the high ablation efficiency of In by the "dopant" laser.

The transmission spectra in Figure 4b showed that AZO films are in general more transparent than IZO films that showed a dramatic decrease of the transmission with increasing the "dopant" laser fluence. Following the same

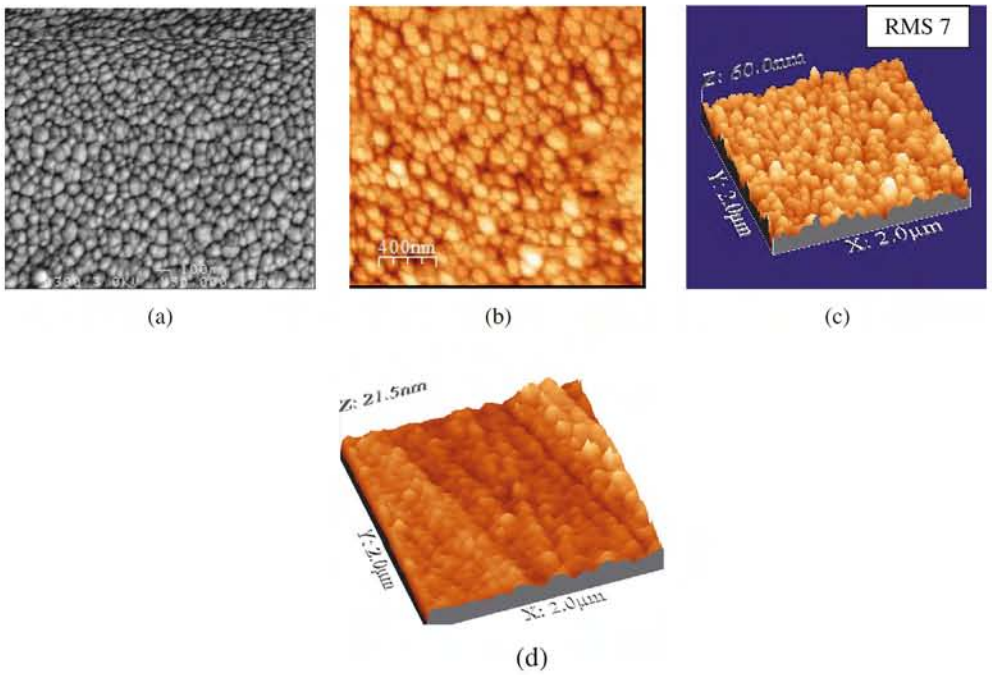

Fig. 3. (Color online) Undoped ZnO sample at 30 Pa: (a) SEM and (b) 2D and (c) 3D AFM micrographs. (d) The 3D AFM image of the PET substrate is shown for comparison.

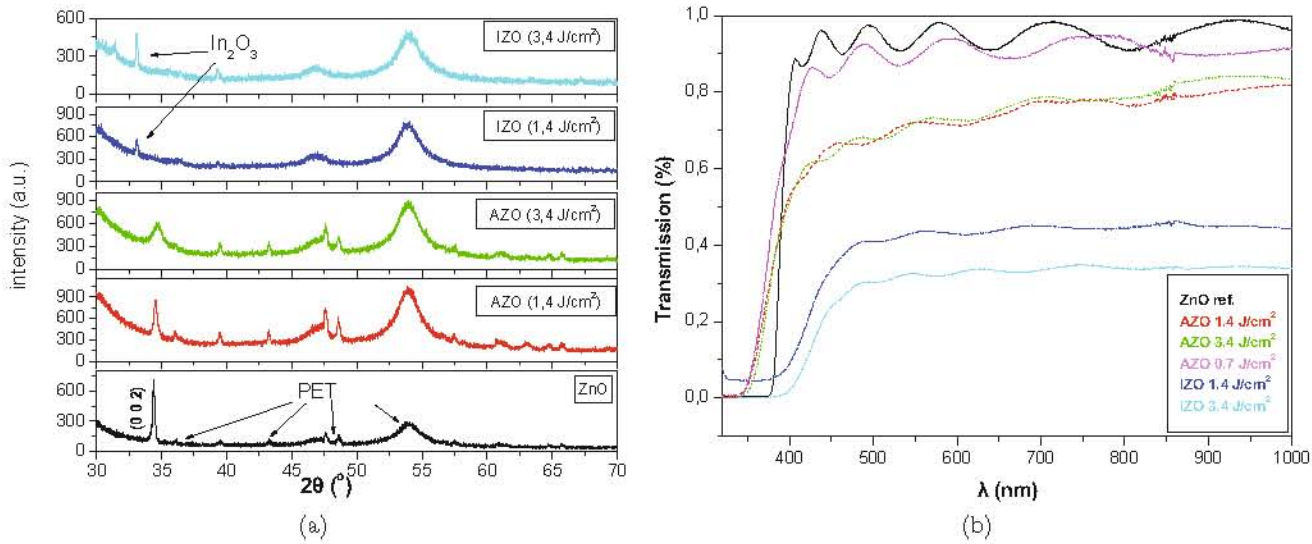

Fig. 4. (Color online) (a) XRD patterns of undoped and Al and In doped zinc oxide films deposited for two fluences of doping laser 1.4 J/cm^{2}and 3.4 J/cm^2, (b) transmission for undoped and Al and In doped ZnO films deposited using different fluences of dopant laser.

The employment of the second "dopant" laser resulted to very different observations for the two dopants. For the Al-doped ZnO (AZO), the crystallinity degrades with the increase of the second laser fluence, as can be seen from the broadening, shifting and decreasing of the (002) ZnO peak. No Al_2O_3 have been observed either. This means that Al is incorporated into the ZnO lattice, replacing Zn sites. We made a similar observation in the past [14]. On the contrary, for the In-doped ZnO (IZO) films, the presence only of the In_2O_3 peaks indicated that the film crystallized rather well as a In_2O_3 matrix that is doped by Zn. This may be the result of the reduced 248 nm laser fluence for the Zn target and the high ablation efficiency of In by the "dopant" laser.

The transmission spectra in Figure 4b showed that AZO films are in general more transparent than IZO films that showed a dramatic decrease of the transmission with increasing the "dopant" laser fluence. Following the same

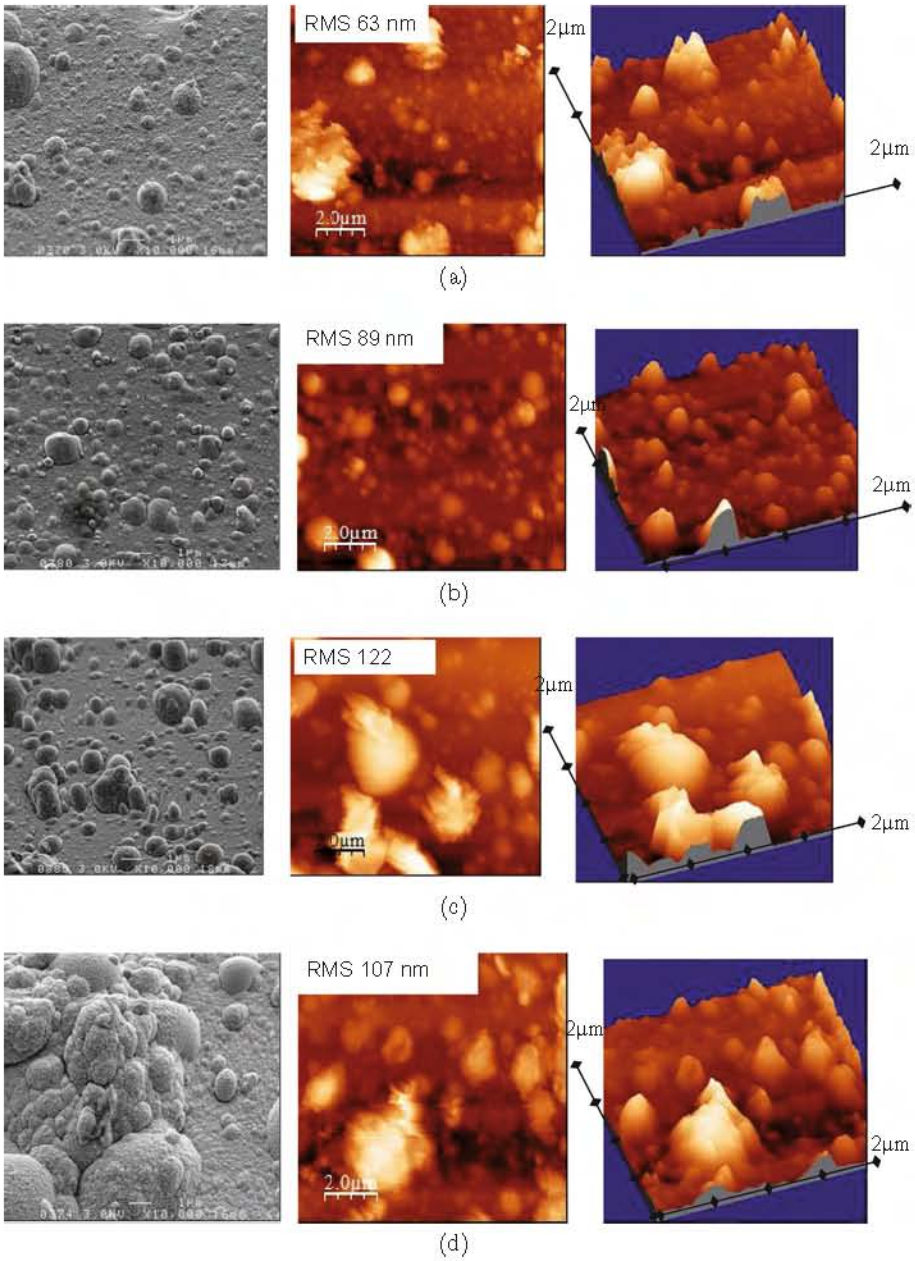

Fig. 5. (Color online) SEM and 2D and 3D AFM images for different "dopant" laser fluence of AZO at (a) 1.4 J/cm^2 and (b) 3.4 J/cm^2, IZO at (c) 1.4 J/cm^2 and (d) 3.4 J/cm^2.

procedure as for the undoped samples above, the thickness of the ZnO reference as well as of 3 AZO films was calculated and is given in Table 2. The thickness values are in average higher than the undoped ones, due to the larger ablation target area for this set of samples. The thickness for the IZO samples is not given, because, as the XRD spectra have indicated an In_2O_3 matrix rather than a ZnO one and therefore the dispersion $n(\lambda)$ for ZnO could not be applied here.

The surface morphological analysis has been performed for all doped samples and the results are presented in Figures 5a and 5b for AZO and IZO respectively. The role of the fluence of the "dopant" laser is very pronounced, in particular for the IZO films grown under the same deposition conditions: surface roughness and μm-sized particulates are significantly enhanced for the IZO films. The reason may be that In is ablated more efficiently, as it has a lower melting point, and is softer than Al. The presence of more and larger μm-sized particulates on the IZO film surface may explain the strong reduction of their transmission because they act as light scattering centres.

In Figure 6, $(\alpha h\nu)^2$ is plotted as a function of the photon energy $(h\nu)$. From these graphs, the optical band gap was calculated according to [15] and the values are listed in Table 2. The AZO films revealed an increase of band

Table 2. Thickness, resistivity and optical band gap values for the doped zinc oxide films (for 2 J/cm^2 of the 248 nm laser).

Sample	$F_{355\ nm}$ (J/cm^2)	Thickness (nm)	Resistivity (Ω cm)	Optical gap (eV)
ZnO (ref.)	–	775 +/− 10	2×10^3	3.22
AZO	3.4	726	1.9×10^2	3.43
AZO	1.4	625	0.17	3.43
AZO	0.7	600	0.11	3.52
IZO	3.4		5.5×10^2	2.97
IZO	1.4		2	2.94

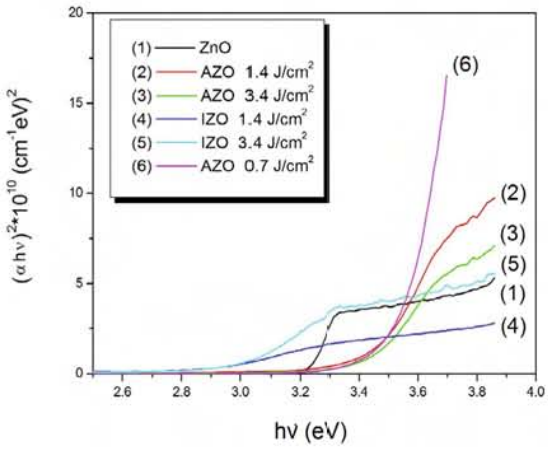

Fig. 6. (Color online) $(\alpha h\nu)^2$ vs. $h\nu$ photon energy plots for films prepared under various conditions, α being the absorption coefficient.

gap with Al as dopant [16]. On the other hand, doping with In caused a decrease of band gap as the transmittance reached the zero at a higher wavelength.

The calculated resistivity values, as determined by the four point method for doped films are also listed in Table 2. From the literature it is known [16,17] that the resistivity of doped ZnO thin films shows a minimum value with the dopant concentration. Table 2 indicates therefore that the optimum "dopant" laser fluence for the lowest resistivity is 0.7 J/cm^2 or less.

4 Conclusions

The R-PLD method allows the growth of semiconducting thin films with good quality on flexible substrates at 120 °C. In this preliminary study, the fluence control of the two employed lasers is crucial for the properties of the grown compound materials. The In doped ZnO thin films, deposited under the present conditions, seem to be inappropriate for photovoltaic applications, due to their low conductivity as well as low transparency induced by the big particulates on their surface. These effects are less pronounced for Al doped ZnO thin films for which both the resistivity and the transparency values that were obtained, indicated that this method is suitable for the deposition of transparent conductive oxides on plastic substrates. It is expected that these properties may further be improved for "dopant" laser fluence less than 0.7 J/cm^2.

References

1. H. Kim, J.S. Horwitz, G.P. Kushto, Z.H. Kafafi, D.B. Chrisey, Appl. Phys. Lett. **79**, 284 (2001)
2. T. Minami, H. Sonohara, T. Kakumu, S. Takata, Thin Solid Films **270**, 37 (1995)
3. J. Ma, S. Li, J. Zhao, H. Ma, Thin Solid Films **307**, 200 (1997)
4. A.K. Kulkarni, T. Lim, M. Khan, K.H. Schulz, J. Vac. Sci. Technol. A **16**, 1636 (1998)
5. M. Rusu, G.G. Rusu, M. Girtan, S. Dabos Seignon, J. Non-Cryst. Solids **354**, 4461 (2008)
6. M. Girtan, S. Dabos-Seignon, G.G. Rusu, M. Rusu, Appl. Surf. Sci. **254**, 4179 (2008)
7. G.G. Rusu, M. Girtan, M. Rusu, Superlatt. Microstruct. **42**, 116 (2007)
8. M.A. Kaid, A. Ashour, Appl. Surf. Sci. **253**, 3029 (2007)
9. K. Ellmer, R. Mientus, Thin Solid Films **516**, 4620 (2008)
10. M. Kompitsas, A. Giannoudakos, E. György, G. Sauthier, A. Figueras, I.N. Mihailescu, Thin Solid Films **515**, 8582 (2007)
11. S. Venkatachalam, Y. Iida, Y. Kanno, Superlatt. Microstruct. **44**, 127 (2008)
12. J.C. Manifacier, J. Gasiot, J.P. Fillard, J. Phys. E: Sci. Instrum. **9**, 1002 (1976)
13. E. Dumont, B. Dugnoille, S. Bienfait, Thin Solid Films **353**, 93 (1999)
14. E. György, J. Santiso, A. Giannoudakos, M. Kompitsas, I.N. Mihailescu, D. Pantelica, Appl. Surf. Sci. **248**, 147 (2005)
15. M. Girtan, G. Folcher, Surf. Coat. Technol. **172**, 242 (2003)
16. H. Kim, A. Piqué, J.S. Horwitz, H. Murata, Z.H. Kafafi, C.M. Gilmore, D.B. Chrisey, Thin Solid Films **377**, 798 (2000)
17. S.H. Geong, B.N. Park, S.-B. Lee, J.-H. Boo, Surf. Coat. Technol. **201**, 5318 (2007)